Maine Geological Survey
Studies in Maine Geology: Volume 1
1988

Seismic Structure of the Earth's Crust Underlying the State of Maine

Alan L. Kafka
John E. Ebel
Weston Observatory
Department of Geology and Geophysics
Boston College
Weston, Massachusetts 02193

ABSTRACT

As part of the Maine seismic refraction experiment conducted in 1984, the U.S. Geological Survey (USGS) detonated a number of explosions in Maine and southern Quebec. In addition to the recordings made by the USGS, these explosions were also recorded by stations of the New England Seismic Network operated by Weston Observatory and by portable instruments installed by Observatory personnel at various locations in northern New England. The seismic structure of the upper crust was studied using an analysis of group velocity dispersion of Rg waves, a tomographic time-term analysis of Pg waves, and an analysis of velocities of direct P waves. Crustal thickness estimates were made using PmP phases. Three regions of differing upper crustal seismic structure were found: (1) a region between the Maine-Quebec border and the central Maine gravity gradient; (2) a region lying to the southeast of the central Maine gravity gradient, extending to and including the area around Penobscot Bay; and (3) the coastal region east of Penobscot Bay. The first region is characterized by mostly small magnitude time-term residuals scattered around zero and by some seismic anisotropy in the northwest. The second region shows strong anisotropy in both the surface waves and the body waves, and generally has larger, positive time-term residuals. The third region has faster upper crustal velocities than those observed in the second region, variable time-term residuals of both positive and negative values, and no observed anisotropy. The thickness of the crust underlying Maine shows some variability, but generally tends to increase from about 33 km along the eastern coast to about 38 km in the northwestern part of the study area. The lateral variation in upper crustal structure delineated by this seismic analysis may elucidate the three-dimensional configuration of lithotectonic terrane boundaries in Maine.

INTRODUCTION

The scale of lateral and vertical variations in earth structure that can be resolved using seismic methods depends upon the wavelength of the seismic waves. Shorter-wavelength energy can be used to resolve smaller features. Determining the details of earth structure using seismic waves requires a high density of sources and receivers as well as the use of the shortest wavelengths (highest frequencies) possible. Where short-wavelength energy is available but dense source/receiver sampling is not, more general information on crustal structure can be achieved with proper data analysis.

The analysis of travel times of body waves and of dispersion of surface waves has classically been used to study the variation of the seismic velocities in the earth as a function of depth (e.g. Bullen, 1963). Recently, experiments utilizing large numbers of sources and receivers in body-wave and surface-wave experiments have led to improved models of the seismic structure of the earth's crust with resolution of lateral as well as vertical velocity variations (e.g. McMechan and Mooney, 1980; Nakanishi, 1985; Suetsugu and Nakanishi, 1985). One important seismic method which is used to investigate the structure of the earth is called tomography (Fawcett and Clayton, 1984). The tomographic method involves using data from a number of crisscrossing paths of seismic waves in a given region to delimit lateral and vertical variations in seismic velocity. Since

tomography is a ray method, it is used with data where the typical wavelength is short compared to the size of the structures being studied. It can be applied to both surface waves (e.g. Nakanishi and Anderson, 1983; Woodhouse and Dziewonski, 1984) and body waves (e.g. Hearn and Clayton, 1986a, 1986b). In this paper, we discuss the analysis of short-period surface-waves ($1.6 \geq T \geq 0.4$ sec) and body-waves ($1.0 > T > 0.1$ sec) recorded in Maine. From the data analysis presented in this paper, we are able to discern variations in the structure of the earth's crust underlying Maine.

In 1984 a seismic refraction experiment was conducted in Maine by the United States Geological Survey (USGS), and this experiment included a large number of explosion sources with known origin times and locations (Murphy and Luetgert, 1986, in press). This refraction experiment was part of a major geophysical investigation of the northern Appalachians in Maine using seismic reflection, seismic refraction, gravity, and magnetic methods (Stewart et al., 1986). Forty-eight refraction blasts were detonated for this experiment. These shots ranged in size from 1600 to 4000 pounds, and they were located at various sites in Maine and southern Quebec. In addition to the recordings made by the USGS, the shots were also recorded by the regional New England Seismic Network operated by Weston Observatory, and by portable stations installed by Observatory personnel (Fig. 1). The Weston Observatory data set complements the USGS data set because it includes many ray paths not sampled by the USGS data set. In this paper, we analyze the Weston Observatory data set recorded from the USGS experiment.

Prior to the 1984 experiment, relatively little work had been done on analyzing the details of the seismic structure of the crust beneath Maine. The crustal structure of southeastern Maine had been studied by Suzuki (1964) using data from the 1961 Gulf of Maine seismic refraction experiment. A crustal model for nearby central New Hampshire had been determined by Taylor and Toksoz (1979). Eichorn (1980) used quarry blasts and portable seismic stations in central and northern Maine to investigate the crustal structure in that part of the state. The crustal model of Chiburis and Ahner (1980), determined for southern New England, has been used successfully at Weston Observatory to locate earthquakes in northern New England, including Maine (Ebel, 1986). Several of the earlier models of the New England crust are shown in Table 1. The models determined from these earlier studies only give information on the average vertical seismic structure of the area and do not elucidate details of lateral variations in velocity or layer thickness. Thus, the 1984 experiment provided an opportunity to greatly expand the knowledge of crustal structure beneath the state of Maine. While a full reduction of the USGS data set has not yet been completed, some results from the refraction and the reflection experiments have already been published (Doll et al., 1986; Green et al., 1986; Klemperer and Luetgert, 1987; Luetgert, 1985a, 1985b; Luetgert and Bottcher, 1987; Luetgert et al., 1986, 1987; Mann and Luetgert, 1985; Spencer et al., 1987; Unger et al., 1987). These results will be discussed below in conjunction with the results of our analysis of the Weston Observatory data set.

METHODS

The Rg Method

The dispersive properties of surface waves can be used to map lateral heterogeneity in the structure of the earth's crust. Kafka and Reiter (1987) analyzed short-period Rayleigh waves (Rg) recorded from the USGS refraction blasts detonated in southern and central Maine. The method used in that study was also used by Kafka and Dollin (1985) to analyze Rg waves recorded from quarry blasts in southern New England, and it is a short-period analogue of methods used to study lateral variation of dispersion of long-period surface waves propagating in the crust and mantle (e.g. Santo, 1965; Nakanishi and Anderson, 1983). These dispersion methods involve measuring the phase and/or group velocity of surface waves propagating over numerous paths from source to receiver or from station to station. The variation in group or phase velocity dispersion from one path to the next implies a variation in earth structure.

The depth of structures resolved by fundamental mode surface waves is directly related to the periods (and hence wavelengths) observed. The USGS blasts studied by Kafka and Reiter (1987) were all 2000 lb blasts, and they did not generate Rg signals beyond about 1.3 sec period in most cases, although occasionally Rg appeared to be present out to almost 1.6 sec. By comparison, the seismograms of quarry blasts in southern New England studied by Kafka and Dollin (1985) and Kafka and McTigue (1985) have Rg signals at periods as great as 2.5 sec with sufficient energy present that group velocity could be measured. The longer-period Rg waves recorded from the quarry blasts are sensitive to variations in crustal structure to depths of about 2.0 to 3.0 km. Because of the more limited period range observed from the Maine refraction blasts, the Rg data discussed

TABLE 1: EXAMPLES OF CRUSTAL MODELS FOR THE NORTHEASTERN UNITED STATES

V_p (km/sec)	Depth to top (km)	Thickness (km)	Region	Reference
5.31	0.00	0.88	Connecticut	Chiburis and
6.06	0.88	12.21		Ahner (1980)
6.59	13.09	21.51		
8.10	34.60			
6.03	0.00	12.0	Maine	Eichorn (1980)
6.60	12.00	21.0		
6.73	34.00	5.0		
7.20	39.00			
5.70	0.00	7.3	Central New	Taylor and
6.30	7.30	18.8	Hampshire	Toksoz (1979)
7.30	26.10	12.9		
8.13	39.00			

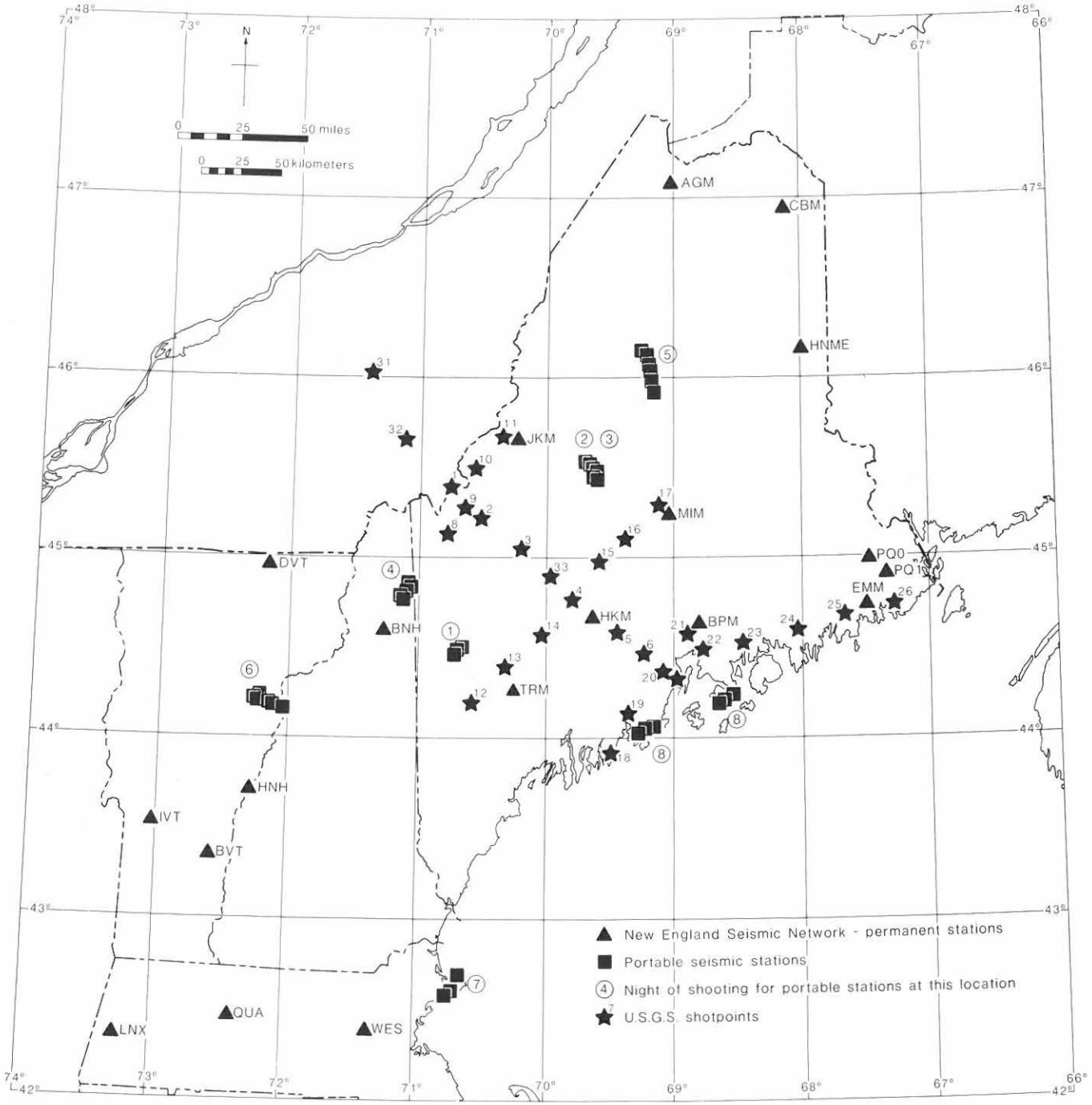

Figure 1. Map of northeastern United States showing stations and shotpoints from this study. Permanent stations of the New England Seismic Network are shown as solid triangles; stars indicate locations of USGS shotpoints (uncircled numbers); and solid squares indicate locations of portable seismic stations deployed for this study. Numbers in circles indicate the night of shooting when portable stations were deployed at a particular location.

here are not very sensitive to variations in crustal structure deeper than about 1.5 to 2.0 km. Within that very shallow portion of the crust, however, Rg dispersion studies reveal details of the seismic velocity structure. Thus, these Rg studies complement the body-wave studies discussed here, since the body-wave studies yield models of deeper portions of the crust.

The Tomographic Time-term Method

Travel times from the first arriving P waves recorded from the USGS refraction blasts were analyzed using the method of Hearn and Clayton (1986a). This method, which we refer to as the tomographic time-term method, is illustrated in Figure

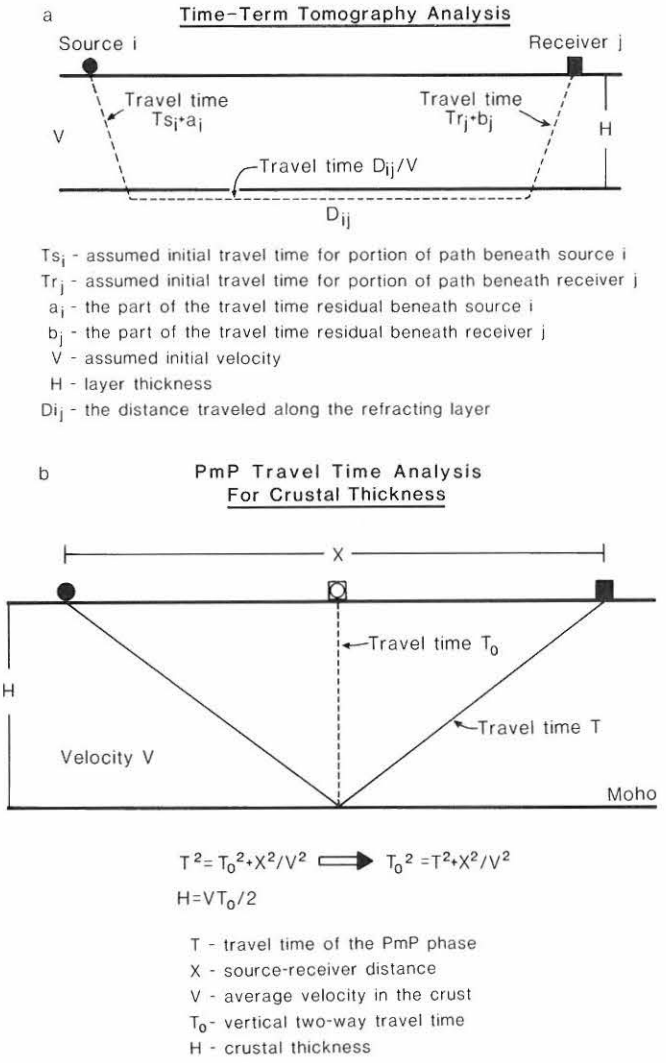

Figure 2. Schematic diagrams of (a) time-term tomography analysis and (b) PmP travel-time analysis.

2a. The travel times are measured for all first arriving P waves which refract as head waves along the top of a particular layer in the crust. The expected travel time calculated from a preliminary layered velocity model of the crust is then subtracted from the observed travel time for each ray path, yielding a travel-time residual. Negative and positive residuals are early and late arrivals, respectively, relative to the preliminary crustal model. The absolute values of the time-term residuals are a function of the initial velocity model used in the analysis.

The refracting layer is divided into a number of blocks, and for each path the resulting travel-time residual is distributed into the crust above the refracting layer beneath the source, the crust above the refracting layer beneath the receiver, and each refractor block. For a large number of source-receiver paths, this leads to the problem of finding a crustal structure that best fits the average residuals for each source position, receiver position, and refractor block. This is an overdetermined problem that can be solved by the least-squares method. The average source and receiver residuals, also called time-term residuals, can be interpreted as resulting from variations of crustal velocities relative to those of the initial model, variations of the depth to the top of the refracting layer, or a combination of both of these effects. The average residual values for the refractor block can be caused by changes in the velocity of the refracting layer, by topography along the top of the refracting layer, or by both effects together. The method is most effective when there are a large number of observations which sample each source, receiver, and refractor block with a number of different source-receiver geometries.

The highest frequency P waves used for the tomographic time-term analysis were about 5 to 10 Hz. This frequency range corresponds to wavelengths as short as 0.6 km. In principle, objects as small as this shortest wavelength can be resolved, but tomographic methods in general act as spatial smoothing filters (Fawcett and Clayton, 1984), and the practical limit on the lateral resolution depends upon the density of source-receiver pairs. In the vertical direction, the depth resolution depends upon the thickness of the crust above the refracting layer as well as upon the thickness and vertical velocity structure within the refracting layer. A positive vertical velocity gradient with depth in the refracting layer will cause longer travel paths to have deeper bottoming points within that layer, and this will affect both the final refractor block residuals and, to some lesser extent, the final time-term residuals computed with the method. Thus, the time-term residuals reflect seismic velocity and layer thickness variations from the assumed model at depths primarily above the refracting layer, while the average block residuals are mainly due to seismic velocity variations within the refracting layer itself.

The PmP Method

The thickness of the crust at different points in Maine was also sampled using the travel times of PmP waves. The PmP phase is a P wave that is reflected from the Moho discontinuity. In Figure 2b we show how the thickness of the crust is sampled by the PmP wave. For surface sources and receivers, the PmP reflection point is approximately halfway between the source and receiver, and the crustal thickness at that point can be estimated from the PmP travel time and an assumed average crustal velocity (Sheriff and Geldart, 1982; Luetgert et al., 1987). This method is approximate since it assumes that the crust can be modeled as a single layer.

The ability of the PmP method to resolve crustal thickness depends upon the accuracy of the average crustal velocity that was assumed in the initial model, the source-receiver distance, and the accuracy of the measured PmP travel times. In this experiment, the source-receiver distances and the PmP travel times are known quite well (assuming, of course, that the PmP phase has been correctly identified), so the accuracy of the crustal thickness estimates hinge primarily upon the accuracy of the average crustal velocity assumed in the initial model. The er-

ror in the crustal thickness values as a function of a given error in the average crustal velocity increases with increasing source-receiver distance. For example, an error of 0.1 km/sec in the average crustal velocity yields crustal thickness errors of 1.7 km and 4.6 km at source-receiver distances of 100 km and 200 km respectively. An assumed average velocity which is slower than that along the ray path will yield crustal depth estimates which are less than the correct depths.

DATA ANALYSIS

Seismic Stations Used for this Study

The locations of the permanent stations of the New England Seismic Network and the portable seismic stations used in this study are shown in Figure 1 along with the USGS refraction shot locations. Each of the New England Seismic Network stations has a 1-Hz vertical seismometer. The data are transmitted via telephone telemetry to Weston Observatory where they are recorded in both analog and digital form. The digital system has a sampling rate of 50 samples/sec for each station (0.02 sec reading accuracy) and a system displacement response that peaks at approximately 10 Hz. The analog data were recorded on two 16 mm photographic recorders. Each photographic unit records 18 stations, and the photographic records can be read to a precision of 0.05 sec. Absolute time is provided by a satellite receiver connected to both the analog and digital systems. A more complete description of the New England Seismic Network instrumentation is given in Ebel (1985).

The portable instrumentation included five smoked-paper recorders and two three-component digital recorders. The smoked-paper recorders were connected to 1-Hz vertical seismometers and were operated at recording speeds of 240 mm/min or 120 mm/min, yielding reading accuracies of 0.02 or 0.04 sec respectively with proper magnification. The digital units recorded all three components of ground motion from 1-Hz seismometers. The sampling rates for the digital units were set to 100 samples/sec. The clocks of the portable instruments were calibrated against the satellite time standard of the New England Seismic Network just prior to their deployment.

Instrumentation failures somewhat reduced the yield of usable data. During the 8 nights of shooting, the digital recording system failed on the fourth night and one of the photographic recorders failed on the first night of shooting. On a given night, only 6 of the shots could be recorded by the New England Seismic Network digital system due to data storage limitations. Digital data were successfully recorded at the New England Seismic Network stations for 44 of the shots. Of the 48 portable field stations deployed, 30 produced records that could be analyzed.

Analysis of Rg Waves

Since the USGS refraction blasts were located at essentially zero depth, they generated fundamental mode Rayleigh waves (Rg) that were recorded at some of the New England Seismic Network stations. Rg data from two New England Seismic Network stations in central Maine (HKM and MIM) were analyzed by Kafka and Reiter (1987), and their data analysis and results are summarized below.

All traces selected for the Rg analysis were first inspected visually for prominent Rg arrivals, and an amplitude spectrum was calculated for each trace. The highest signal-to-noise ratio for Rg waves recorded from the refraction blasts was generally in the period range of about 0.3 to 1.3 sec. Seismograms that had strong signals in that period range were examined, and for those seismograms the background noise was also analyzed to ensure that it did not overlap severely with the Rg signal. Based on this preliminary screening of the data, twelve paths were chosen for the dispersion analysis.

To illustrate the Rg methodology used by Kafka and Reiter (1987), we show their analysis for one of the better examples of Rg data recorded from the Maine refraction shots (Fig. 3). The upper trace in Figure 3a is the seismogram recorded at station HKM from shotpoint #6, and the lower trace is the same seismogram after being low-pass filtered. The prominent dispersed wave train arriving between about 7 and 12 sec is the Rg wave. Figure 3b shows the amplitude spectrum of the original recorded trace. In that figure, the prominent spectral peak centered at about 2 Hz corresponds to the Rg wave. This peak is characteristic of Rg waves recorded by the New England Seismic Network from surface blasts and very shallow earthquakes.

Group velocities of Rg waves from the Maine refraction blasts studied by Kafka and Reiter (1987) were measured using the technique of narrow-band pass filtering (Dziewonski et al., 1969). The result of applying the narrow-band pass filter analysis to the seismogram from shot #6 recorded at station HKM is shown in Figure 3c. The seismogram is Fourier transformed and narrow-band pass filtered about a series of center frequencies. For each center frequency, the group arrival time is approximated by measuring the arrival time of the maximum amplitude of the envelope of the filtered signal. This process is repeated for a series of center frequencies, and group velocities are estimated at each center frequency. Group velocities, determined using the narrow-band pass filter analysis, are shown in Figure 4 for all twelve paths analyzed.

The group velocity dispersion curves shown in Figure 4 were inverted by Kafka and Reiter (1987) using a linearized least squares method (Backus and Gilbert, 1970; Der et al., 1970; Franklin, 1972) to determine the velocity structure of the shallow crust underlying the twelve paths analyzed. Similar methods have been used extensively to invert longer-period surface waves for deeper structures (e.g. Mitchell and Herrmann, 1979; Taylor and Toksoz, 1982). Since Rayleigh waves are most sensitive to shear wave velocity, the shallow crustal models determined from this inversion are essentially shear wave velocity models. To compare the Rg inversion results with seismic velocities determined from the body wave analyses, it is necessary to estimate V_p. Kafka and Reiter used a V_p/V_s ratio of 1.78 to convert S-wave velocities to P-wave velocity estimates. Later in the report we discuss the compatibility of the

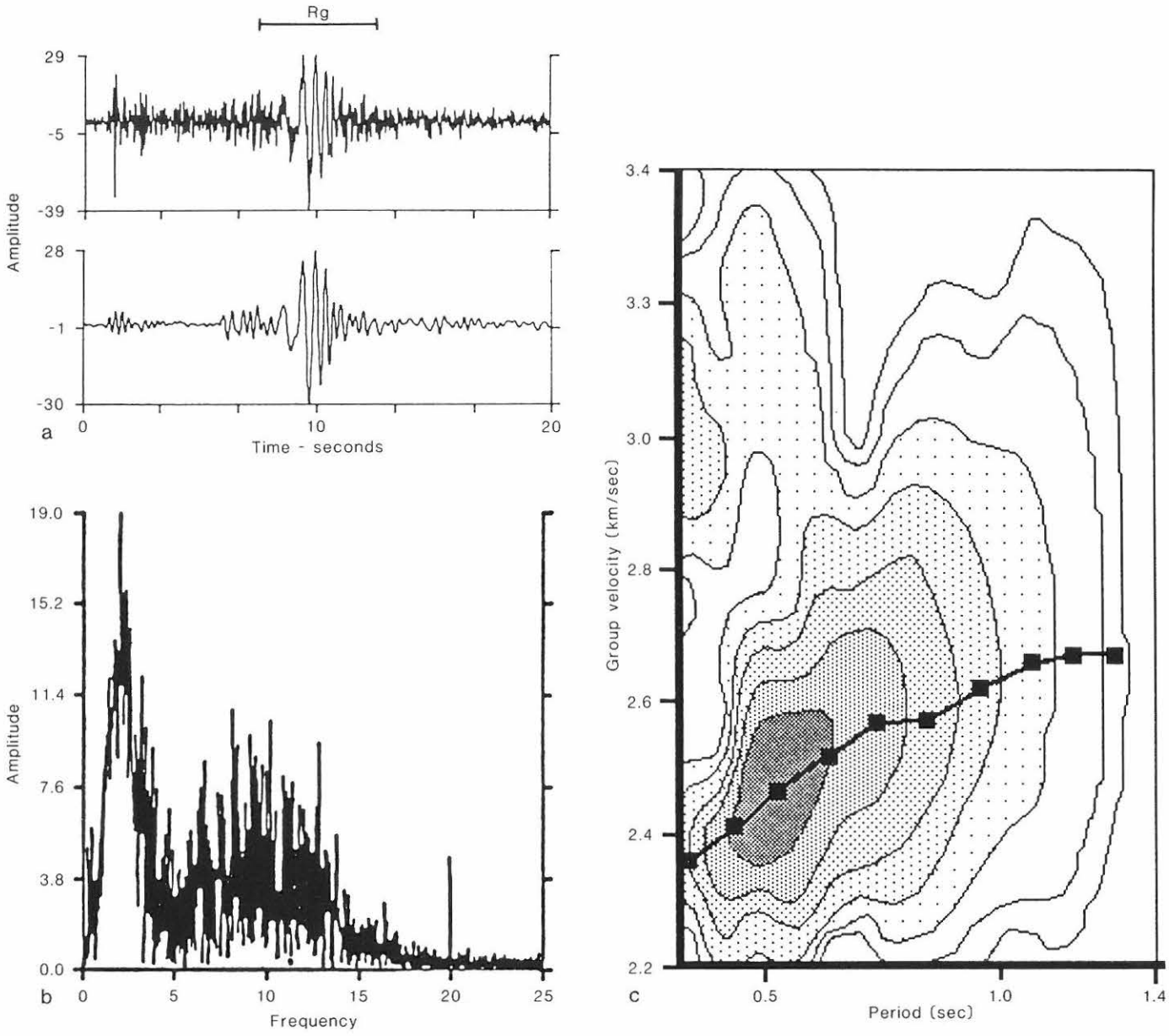

Figure 3. Example of Rg waves recorded from one of the USGS blasts and illustration of Rg methodology. (a) Upper trace is the seismogram recorded at a distance of 39 km from a 2000 lb blast. Below is a low-pass filtered trace with a high-frequency cutoff of 4 Hz. (b) Amplitude spectrum of the raw seismogram (upper trace) shown in (a). The prominent peak at about 2 Hz is characteristic of Rg waves recorded by the New England Seismic Network. (c) Narrow-band pass filter analysis of the seismogram shown in (a). Each contour interval represents a change of 2 db in the amplitude of the filtered signal envelope at a given center frequency.

surface wave and body wave results for a range of V_p/V_s values.

Analysis of Body Waves

Tomographic Time-term Analysis. The tomographic time-term method was applied to two separate data sets read from the New England Seismic Network records: first arrivals representing the Pg phase (a head wave in the upper crust with an apparent velocity of about 6.1 km/sec) and those representing the Pn phase (a head wave in the uppermost mantle with an apparent velocity of about 8.1 km/sec). All first arrival times for source-receiver distances of 30 km to 160 km were assumed to be the Pg phase, and first arrivals at distances beyond 190 km were assumed to be the Pn phase. These distances were chosen based on the calculated crossover distances for the Chiburis and Ahner (1980) crustal model as well as on a preliminary analysis of the USGS refraction observations (J. Luetgert, pers.

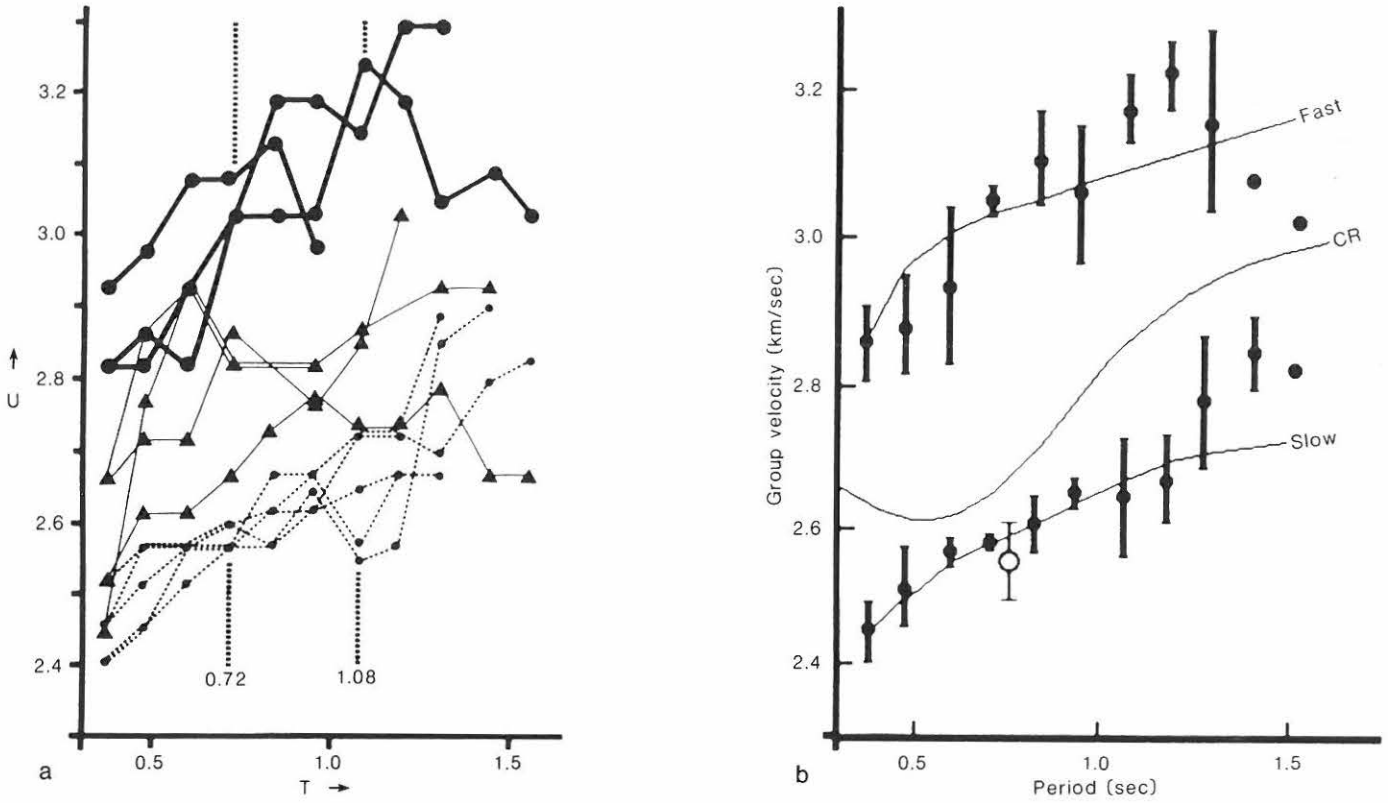

Figure 4. (a) Group velocity data for Rg waves recorded by stations HKM and MIM. Thick solid lines, narrow solid lines and dotted lines represent fast, intermediate and slow clusters respectively. U is group velocity in km/sec, and T is period in sec. (b) Average and standard deviation of Rg group velocities for slow and fast clusters shown in (a). The open circle corresponds to a peak-and-trough measurement for blast #20 to HKM. Also shown are dispersion curves for shallow crustal models of the region surrounding stations HKM and MIM along with the dispersion curve corresponding to the Chiburis and Ahner (1980) refraction model (curve labelled CR). The shallow crustal models corresponding to the theoretical dispersion curves are shown in Figure 6.

commun., 1984). No portable instrument data were used in this particular analysis.

The travel times for all shot-receiver pairs with clear first arrivals were read from both the analog and the digital New England Seismic Network records, and travel-time residuals for each path were then computed relative to the Chiburis and Ahner (1980) model. The set of residuals at each station was then examined. Some shotpoints had been reused as many as 6 times, and for each of these shotpoints the travel-time residuals for different paths could be compared and the most appropriate residual selected. In general, the largest shot at a given shotpoint gave the most reliable travel-time readings. Next, the travel-time residuals from adjacent shotpoints to a given station were examined. Residuals that differed significantly from those corresponding to other nearby shotpoints were discarded. In all cases where it existed, the readings from the digital data were given preference over the analog readings. In the last step, each selected travel-time residual was assigned a weighting factor based on the reading precision and quality and on the shot size. The final data sets for the Pg and Pn analyses had 153 and 57 different travel paths respectively.

The refractor layers were divided into a number of different blocks. The blocks were chosen to be sufficiently large to collect a good sampling of rays, but small enough to resolve some lateral heterogeneity. For the Pg refractor, the blocks were about 52 km by 54 km in lateral extent, while for the Pn refractor they were about 75 km by 78 km. Travel distances for each ray in each block were computed by hand and stored along with the path identification, travel-time residual, and path weight in a computer file. The data sets were then inverted using the least-squares procedure of Hearn and Clayton (1986a) to get the average residuals at each shot and receiver point for each refractor block. The refractor block residuals were converted to refractor velocity perturbations (Hearn and Clayton, 1986a), and new velocitites were found for each refractor block.

PmP Analysis. For the PmP crustal thickness analysis, the relatively wide spacing between individual receivers as well as between individual shotpoints made the recognition of the true PmP phase on most records difficult. However, Nutting (1984) showed that, for the Chiburis and Ahner (1980) crustal model, the PmP phase has a very large amplitude beyond 90 km (a distance where it becomes post-critical). Between about 90 km and

120 km, PmP is noticeably separated in time from other major crustal reflections and refractions. From 120 km to about 200 km, PmP arrives very close in time to other P phases that reflect and refract in the middle of the crust. Beyond 200 km, PmP again becomes separated in time and easier to identify. All of the records (New England Seismic Network and portable) were scanned for possible PmP phases, with special attention being paid to the distance range of 90 km to 120 km and to distances beyond 200 km. All phases with amplitudes noticeably above the surrounding signal and with travel times near that expected for PmP were selected and read. Only 39 readings out of 129 seismograms were considered reliable. Crustal thickness values were then computed from the final set of PmP travel times, and the resulting value for each path was assigned to a point midway between the source and receiver.

RESULTS

Rg Wave Results

In the period range analyzed (0.4 to 1.6 sec), Kafka and Reiter (1987) observed Rg group velocities ranging from about 2.4 to 3.3 km/sec (Fig. 4). As in other studies of Rg dispersion, they observed normal dispersion at shorter periods. This normal dispersion indicates that seismic velocities are relatively low in the upper 0.5 to 1.0 km of the crust beneath the region surrounding stations HKM and MIM. The results of their study indicate that in the region investigated, the average V_p increases from about 4.9 km/sec very near the surface, to about 6.2 km/sec at a depth of about 2 km. The total range of observed group velocities (about ± 0.3 km/sec) is similar to that observed by Kafka and Dollin (1985) for Rg waves in southern New England (about ± 0.4 km/sec). The Rg dispersion results shown in Figure 4 were divided into three clusters based on the velocities observed in the period range of 0.72 to 1.08 sec. These three clusters are characterized by *fast, intermediate,* and *slow* group velocities.

Figure 5a shows the paths of Rg waves from Kafka and Reiter's study superposed on a geologic map of southeastern Maine. A simplified model of the structural grain in that region is shown in Figure 5b where the arrows indicate the orientation of the structural grain. Because the grain changes orientation across the region, our simplified model consists of two subregions with different orientations. The observed group velocities appear to depend primarily on the azimuthal orientation of the path relative to the trend of the structural grain. Paths that are transverse to the grain tend to be in the slow cluster, and the three paths that are approximately parallel to the grain are in the fast cluster. Also, paths that are in the intermediate cluster tend to be oblique to the grain. Because of the distribution of paths sampled and the complexity of the geology, it is difficult to unambiguously distinguish between this apparent lateral anisotropy and lateral inhomogeneity in the shallow crust beneath this region. Nonetheless, lateral anisotropy in the shallow crust provides a simple explanation of the observed pattern of Rg dispersion.

The Rg inversion results of Kafka and Reiter (1987) are shown in Figure 6. The average shallow crustal model in Figure 6a is the result of inverting the mean of Rg group velocities for all paths and all periods analyzed by Kafka and Reiter (1987). The data corresponding to that model are shown in Figure 6b. The shallow crustal model resulting from the inversion of the Rg data from the slow cluster is also shown in Figure 6a. Using the V_p/V_s ratio of 1.78 (which was assumed by Kafka and Reiter, 1987), the upper 1.2 km of the slow cluster model is characterized by V_p ranging from 4.8 km/sec very near the surface to 5.4 km/sec at 1.2 km depth. Below 1.2 km, the slow cluster model is characterized by V_p of 5.6 km/sec. In Figure 6c, we show how variation in the assumed V_p/V_s ratio affects the V_p estimates, and we compare those estimates with the reflection and refraction results of Klemperer and Luetgert (1987) for essentially the same path (shotpoints 4, 5, 6, 20, and 7).

The data quality, range of periods observed, and number of paths for the intermediate and fast group velocity clusters were insufficient for a formal inversion. It is clear, however, that to match the group velocities observed for the fast paths, much higher seismic velocities are necessary in the upper 1 to 2 km. Average values for the fast paths are shown in Figure 4b, and a model corresponding to the fast dispersion curves is shown in Figure 6a. The "fast" model shown in Figure 6a was obtained by increasing the velocities in the layers of the "average" model until the calculated dispersion curve approximated the group velocities observed for the fast cluster.

Body Wave Results

Results of Time-term Analysis. The tomographic time-term analysis was applied to the Pg data a number of times, each with a different assumption about the station weights and/or with all refractor block velocities frozen at 6.06 km/sec (the upper crustal velocity of the Chiburis and Ahner (1980) model, which was the only model tested). In these runs, the relative pattern of the time-term residuals was stable, although there was variation in the absolute time-term residuals. Because of the timing limitations of the recording system, time-term variations on the order of 0.05 sec or less are considered unresolvable. For many of the shot or receiver locations, the variations in the time-term residuals among all the runs was 0.05 sec or less. For some of the locations with the largest residuals (either positive or negative) the variations of the time-term residuals calculated among the different runs were as large as 0.4 sec. The run with the originally assigned weights and with the variable refractor block velocities was considered the most reliable. All time-term residuals from that run were near the mean of those values found for all the different test assumptions. It should be noted that this tomographic time-term analysis does not take into account any anisotropy in the upper crust. At those shot and receiver points where significant anisotropy may exist (see

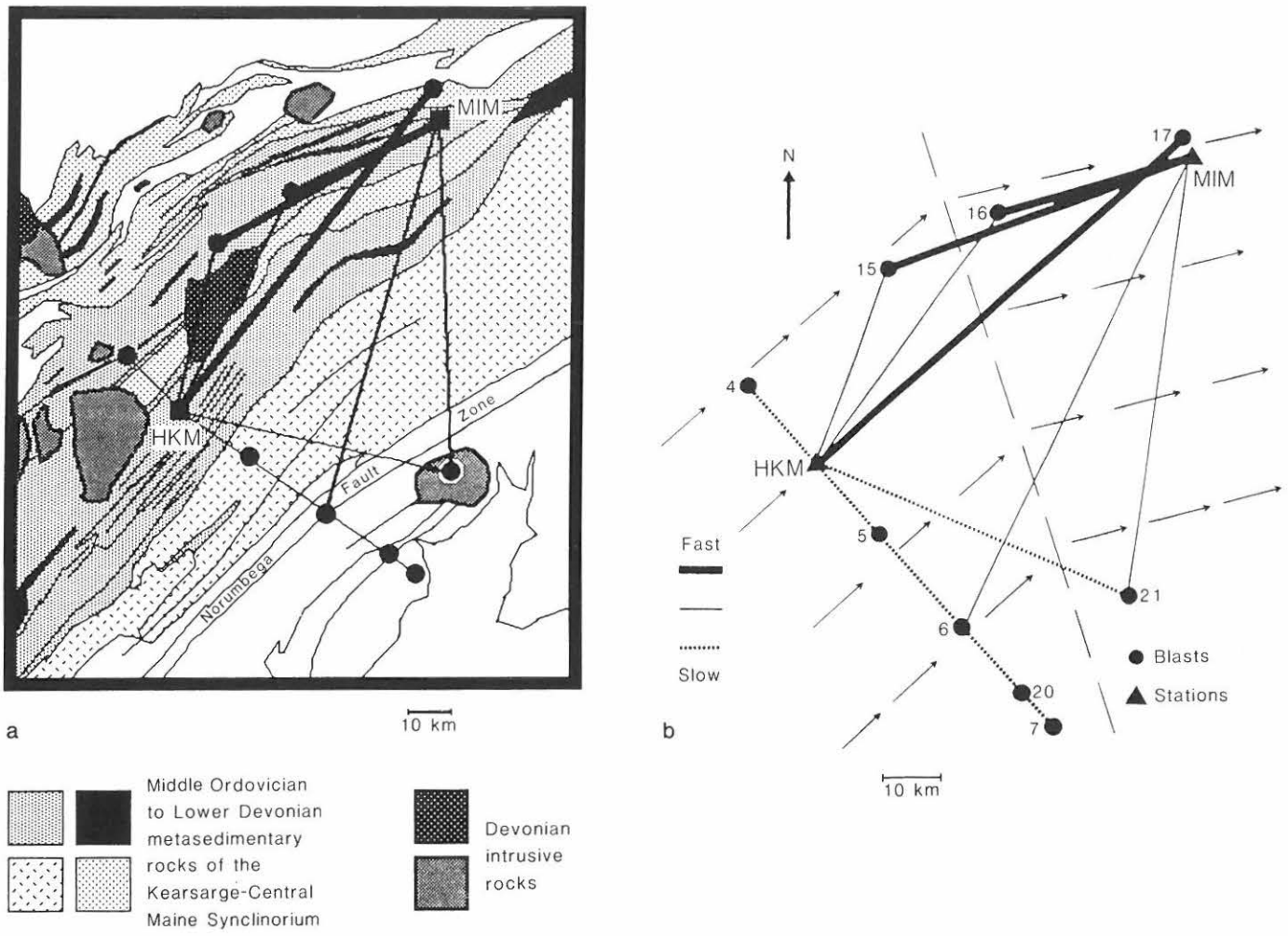

Figure 5. (a) Paths of Rg waves discussed in the text, superposed on a map of geologic structures adapted from the Bedrock Geologic Map of Maine (Osberg et al., 1985). The Norumbega fault zone is labeled NFZ. Closed circles represent refraction blasts, and closed squares represent stations MIM and HKM. (b) Simplified model of the pattern of Rg wave group velocities and the structural grain in the vicinity of stations HKM and MIM. Thick solid lines, narrow solid lines, and dotted lines represent fast, intermediate, and slow paths respectively. For these paths Rg group velocities range from 2.6 to 3.2 km/sec at periods near 1 sec. Arrows represent a simplified model of the orientation of the structural grain.

above and below as well as Doll et al., 1986; Klemperer and Luetgert, 1987), the time-term residuals represent an average travel-time residual which is weighted by the orientations of the observed ray paths relative to the direction of the fastest and slowest velocities. It is because of the variability and uncertainty of the spatial extent of the anisotropy in Maine that it was not included in the tomographic time-term analysis.

The results of the tomographic time-term analysis for the Pg phase are illustrated in Figure 7. All of the shotpoint and receiver time-term residuals are shown, along with a contoured interpretation of those values. Only two refractor blocks were found to have slowness values resolvably different from that of the initial crustal model, and those two blocks along with their calculated velocities are also indicated in Figure 7. In general, the shotpoints in Canada have negative time-term residuals. For the area of northwestern Maine and northern New Hampshire, the time-term residuals are relatively small, ranging from -0.08 sec to 0.16 sec. Between shotpoint 4 and station HKM there is an abrupt change in the time-term residuals to quite large positive values, ranging up to 0.36 sec. This region of large, positive time-term residuals appears to surround Penobscot Bay, extending from HKM southeast to the coast and from shotpoint 18 to shotpoint 22. In this area, the one resolvably slow refractor block, with a velocity of 6.00 km/sec, was found. To the east, the time-term residuals again become negative in the area where the one resolvably fast block (velocity of 6.13 km/sec) is located.

The scatter in time-term residuals between adjacent points is in some cases quite large. In particular, shotpoint 13 was found to have a time-term residual of -0.41 sec, a much more negative value than that for nearby shotpoints or station TRM. An examination of the data used for shotpoint 13 revealed that, while most of the residuals scatter just above or below 0.0, there was

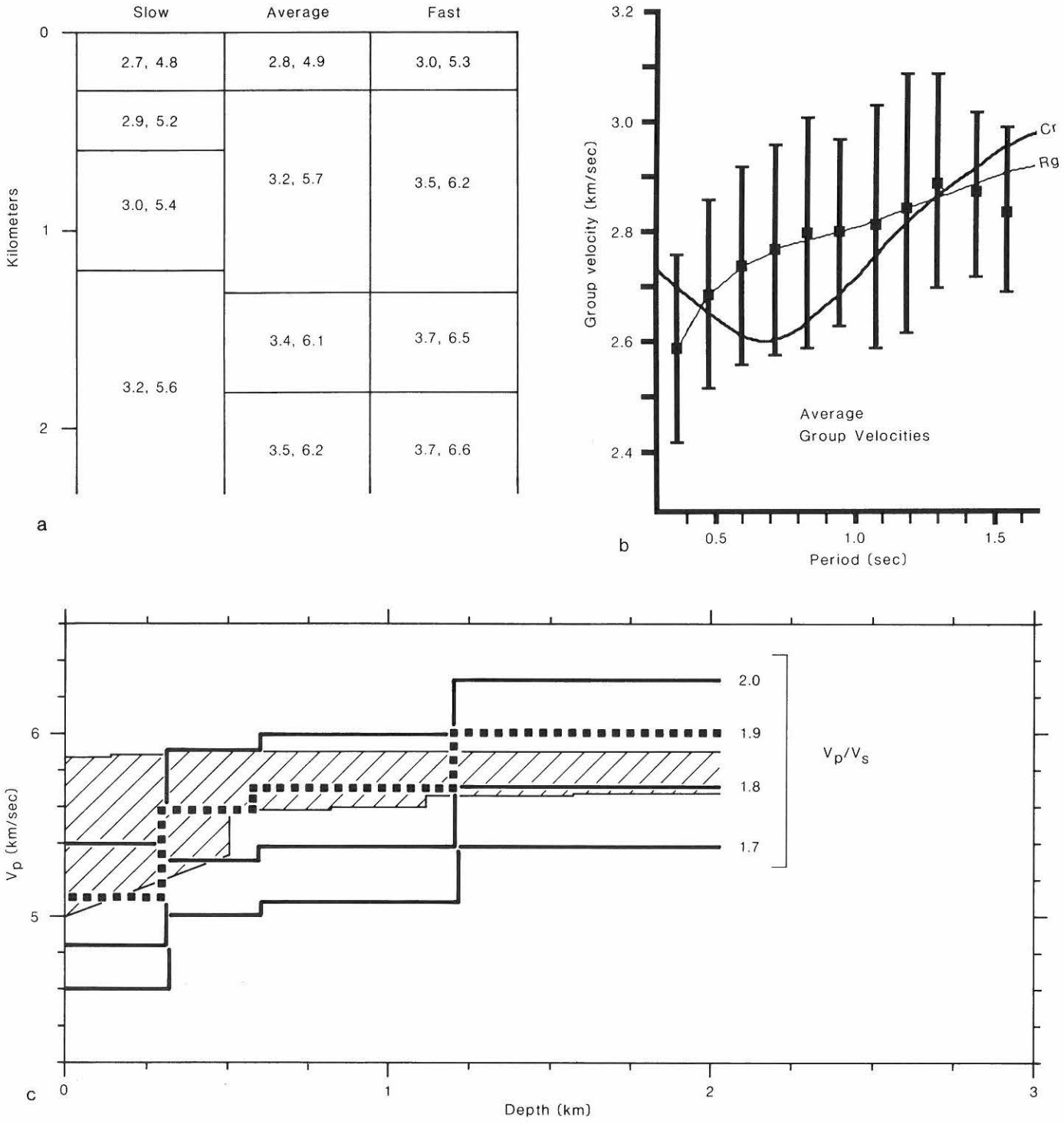

Figure 6. (a) Shallow crustal models determined from Rg dispersion data (from Kafka and Reiter, 1987). Numbers in layers represent V_s and V_p respectively in km/sec. (b) Average and standard deviation for all Rg group velocities shown in Figure 4. Also shown are theoretical dispersion curves corresponding to Chiburis and Ahner (1980) refraction model (CR) and the model resulting from inversion of the Rg data shown here [curve labelled Rg – average model shown in (a)]. (c) Comparison of Rg wave results for the slow paths (solid and dashed lines) with body wave refraction results of Klemperer and Luetgert (1987) (cross-hatched area) for a range of V_p/V_s values.

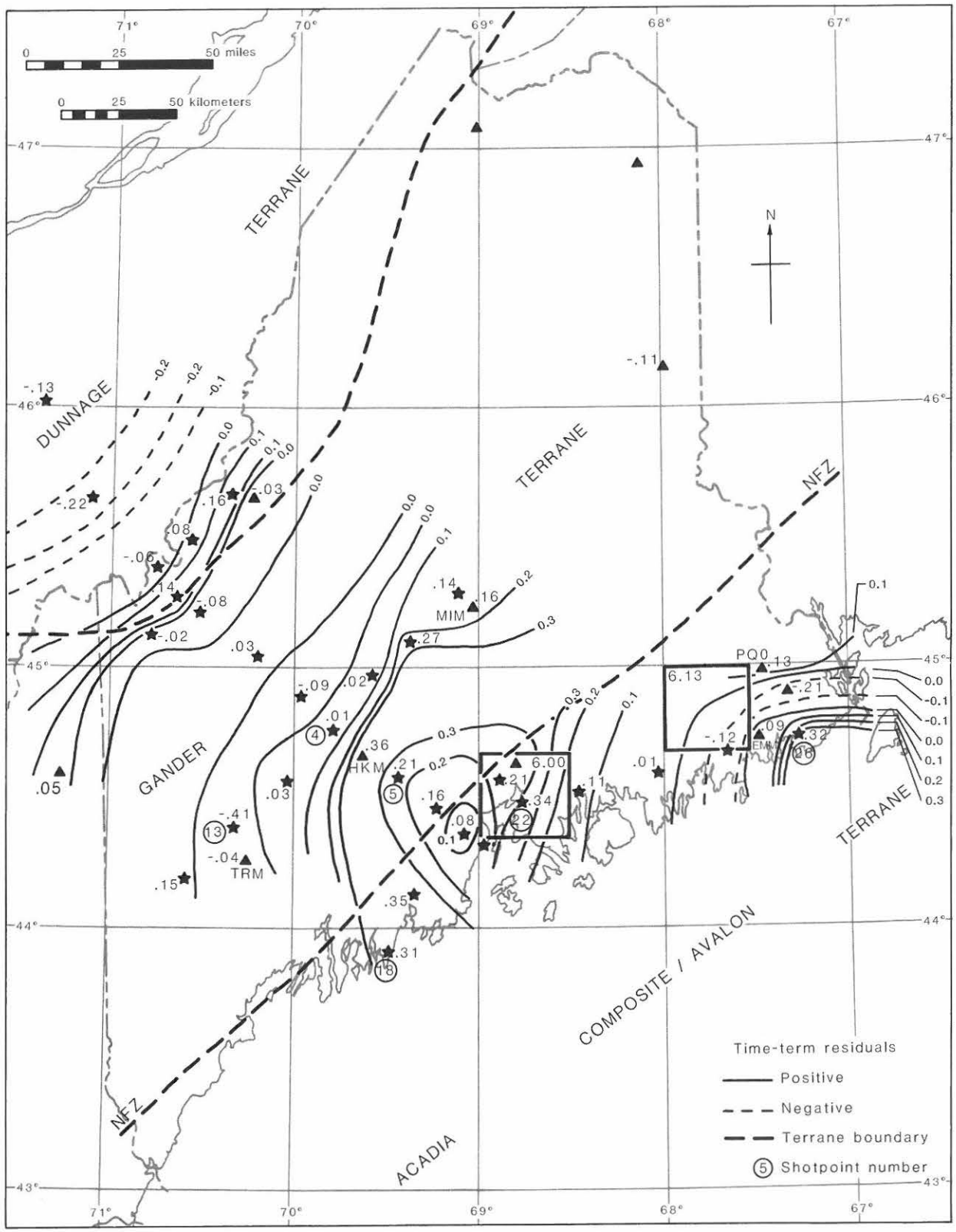

Figure 7. Results of tomographic time-term analysis of Pg waves recorded from the USGS refraction blasts. Numbers next to shotpoints and stations are time-term residuals in sec. Also shown are the boundaries (heavy dashed lines) of the Dunnage, Gander, and Acadia Composite/Avalon terranes discussed in the text. Outlined areas are refractor blocks with resolvably different slowness values.

one travel-time residual on the path to HKM which was very negative (-0.56 sec) and controlled the absolute value of the time-term residual for that point. Shotpoint 26 also appears to have an anomalous time-term residual (0.32 sec) compared to the values found at EMM and PQ0 (0.09 sec and -0.21 sec respectively). However, that time-term residual is consistent with the input data and probably is caused by local structure under the shotpoint, as will be discussed later. The strong change in the time-term residuals between shotpoint 5 and HKM is also considered real from both an examination of the input data and from the consistency of the time-term residuals to the northwest and southeast of this locality.

The application of the tomographic time-term method to the Pn data did not yield reliable results. Time-term residuals ranging from -0.89 sec to 2.04 sec and Pn refractor velocities between 7.61 km/sec and 8.34 km/sec were obtained from the analysis. Adjacent shotpoints or receiver points had radically different time-term residuals in several cases. The low redundancy of the data (most shotpoints and receivers had only 1 or 2 usable data points) was most likely the cause of the problems in this part of the analysis. Even with the poor results of the Pn analysis, however, some of the patterns in the time-terms found in the Pg analysis (for example the region of positive residuals southeast of HKM) appear to have an expression in the Pn results.

Results of PmP Analysis. The PmP analysis yielded a widely-spaced sampling of crustal thickness measurements across the study area (Fig. 8). The same average velocity of 6.4 km/sec was used in a single layer crustal model (Luetgert et al., 1987) for the calculation of all crustal depths shown in Figure 8. It is instructive to compare the results shown in Figure 8 with the results of Luetgert et al. (1987) who were able to use a dense sampling of PmP phases to estimate crustal thickness throughout much of the study area. Along the coast of eastern Maine, a crustal thickness of about 33 km was found in both studies. In northwestern Maine the values found in this study appear to scatter around those reported by Luetgert et al. (1987) for that region. Both studies show a depression in the Moho depth beneath southwestern Maine, although Luetgert et al. (1987) report PmP travel times consistent with a crustal thickness of about 35-36 km beneath that area, whereas thickness values up to 44 km were found in this study. Measurements made in the northern and northeastern part of the area show the greatest discrepancies between the two studies. Luetgert et al. (1987) find thin crust east of shotpoint 17, while Figure 8 shows a quite thick crust there. West of shotpoint 17 we find crustal thickness values around 35 km, while the analysis of Luetgert et al. (1987) is more consistent with 38 km in that area.

Some of the discrepancies between our results and those of Luetgert et al. (1987) can be qualitatively explained. First, most of the crustal thickness estimates that were made from phases recorded at distances of 180 km or more (the underlined values in Fig. 8) yield values which are greater than those expected from the Luetgert et al. (1987) results. Since the PmP phase at this distance range travels a larger percentage of its path in the lower crust than does PmP at distances of 80 km to 120 km, the average crustal velocity necessary to reduce these large distance measurements may need to be greater than 6.4 km/sec. As was noted earlier, small changes in this velocity parameter can affect crustal thickness estimates by several kilometers at distances greater than 200 km. It is also possible that the PmP phase was misidentified at these large distances, since all signals from these blasts had rather low amplitudes on the Weston Observatory records. Second, Luetgert et al. (1987) show that a sizable reflection from a velocity discontinuity in the mid-crust precedes PmP by about 2 sec in the distance range from 89 to 120 km. Thus, some of our crustal thickness values which are less than those expected from the results of Luetgert et al. (1987) may be due to a misidentification of the mid-crustal reflection as PmP. Synthetics calculated by Luetgert et al. (1987) show no significant arrivals within several seconds after the PmP phase in the 89 to 120 km distance range. This makes it problematical to argue that our crustal thickness values that are greater than those of Luetgert et al. (1987) at distances less than 120 km are due to PmP misidentification.

In general, the crustal thickness results from this study support the following principal conclusions of Luetgert et al. (1987): (1) the crust is thinnest under coastal Maine and thickens inland, and (2) there appears to be a depression of the Moho under southwestern Maine. One data point under the White Mountains of central New Hampshire suggests the possibility of thicker crust in that area.

Compatibility of Surface Wave and Body Wave Results

The Rg surface-wave method constrains the seismic structure in very shallow portions of the crust, and the body-wave methods used here generally constrain the structure in deeper parts of the crust. We can test the compatibility of the surface-wave results with the body-wave results by using travel times of the initial P waves to calculate the average velocity for short travel paths which sample shallow portions of the crust. This is done by taking a given shot-receiver distance and dividing that distance by the travel time of the initial P wave. The average velocities for all paths less than about 30 km long are shown in Figure 9. It must be kept in mind that if the velocity is increasing with depth, then the longer the source-receiver distance, the deeper the energy bottoms in the earth. For the paths illustrated in Figure 9, it is likely that the energy bottoms within the upper 2 or 3 km and that the average velocity most closely matches the velocity at and just above the bottoming point of the ray.

Several points can be noted by examining Figure 9. First, the anisotropy pattern noted in the surface wave analysis and by Klemperer and Luetgert (1987) appears to have some expression in the average P wave velocities in the vicinity of stations MIM and HKM. The fast, intermediate, and slow surface wave paths have essentially the same pattern as the P wave average velocities. Second, the average velocities calculated from

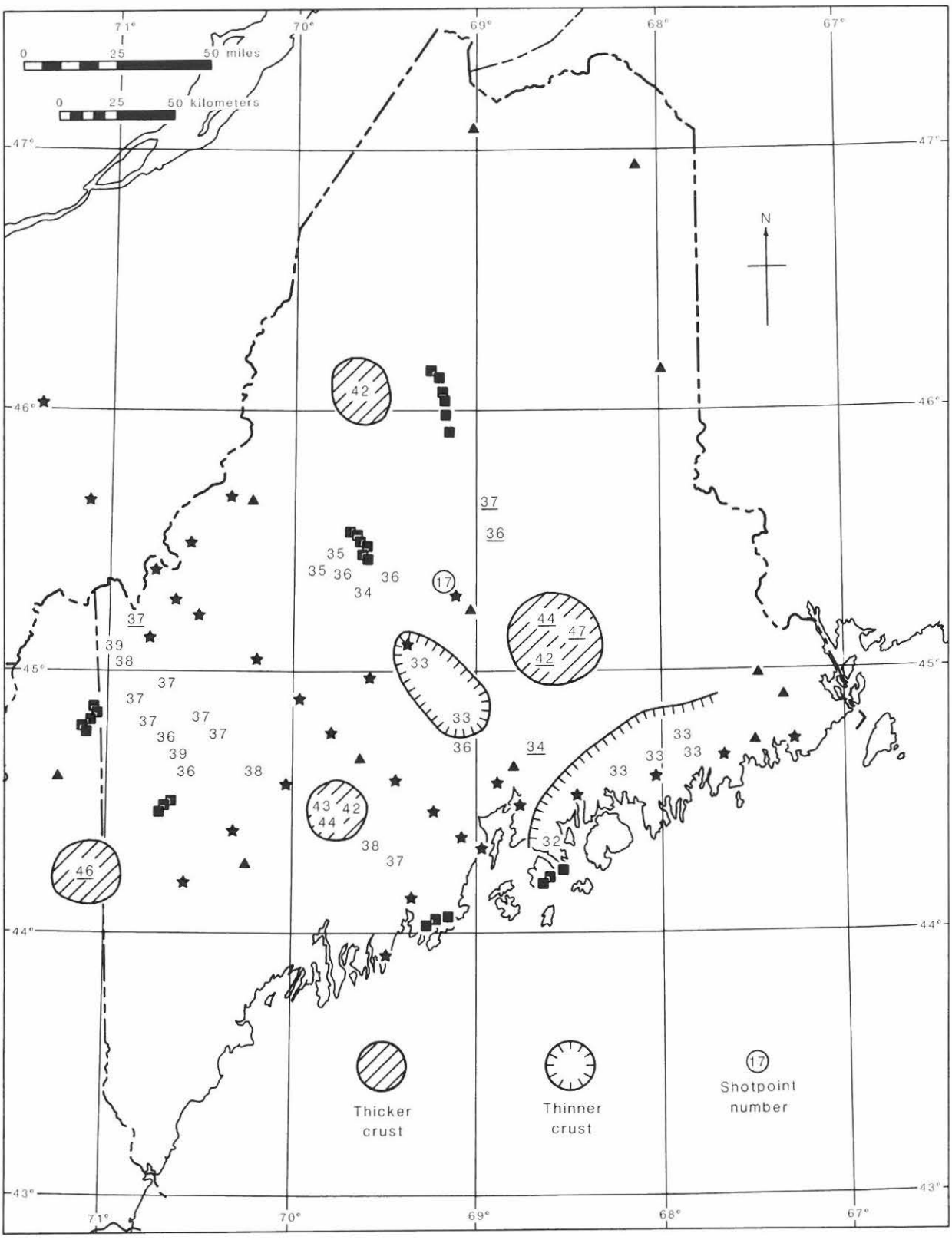

Figure 8. Results of PmP crustal thickness analysis. The crustal thickness estimated for each path was assigned to a point midway between the source and receiver. The underlined values are from shot-receiver distances greater than 180 km.

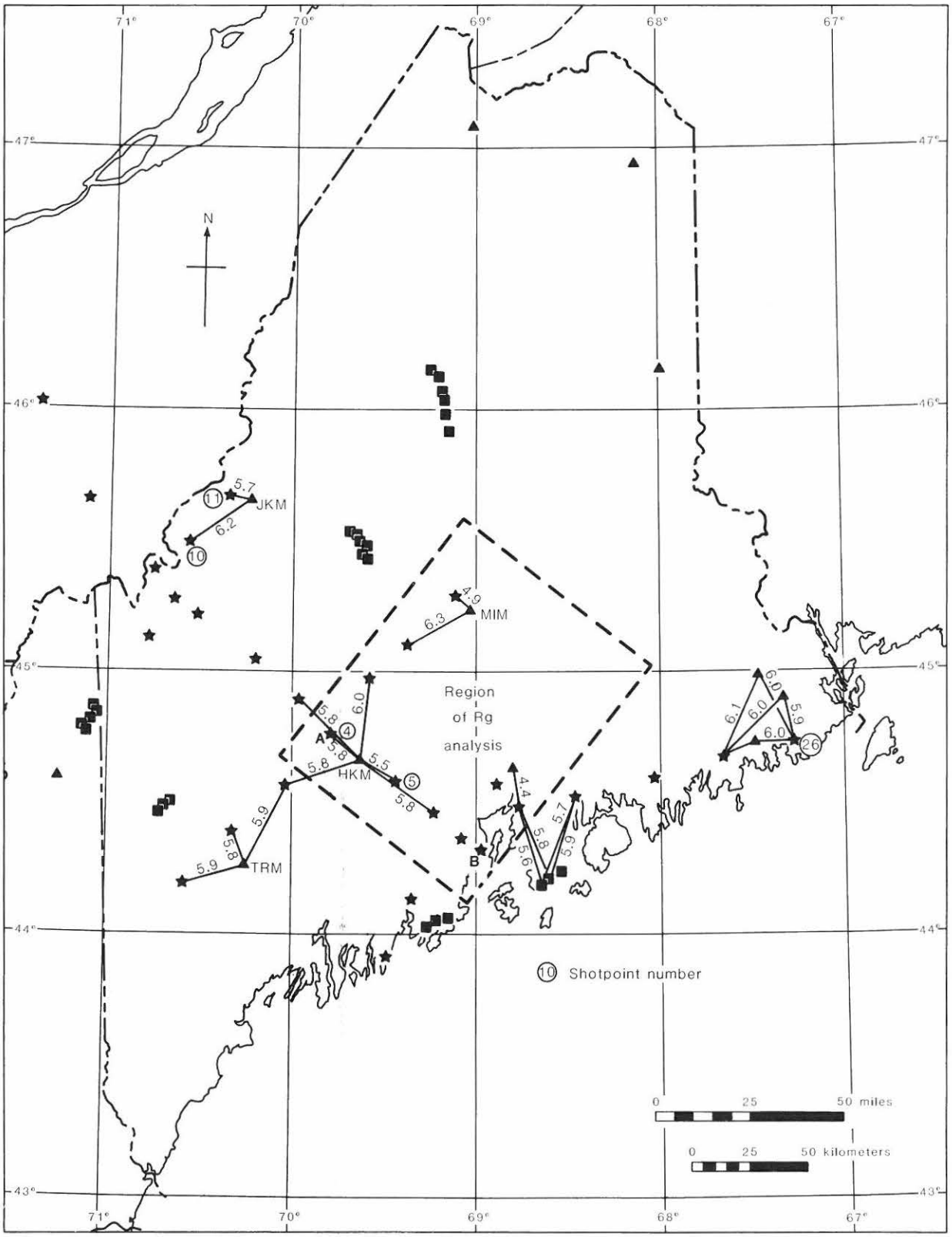

Figure 9a. Average P-wave velocity determined from the travel times of first arrivals of P waves divided into the source-receiver distance for short paths (< about 30 km).

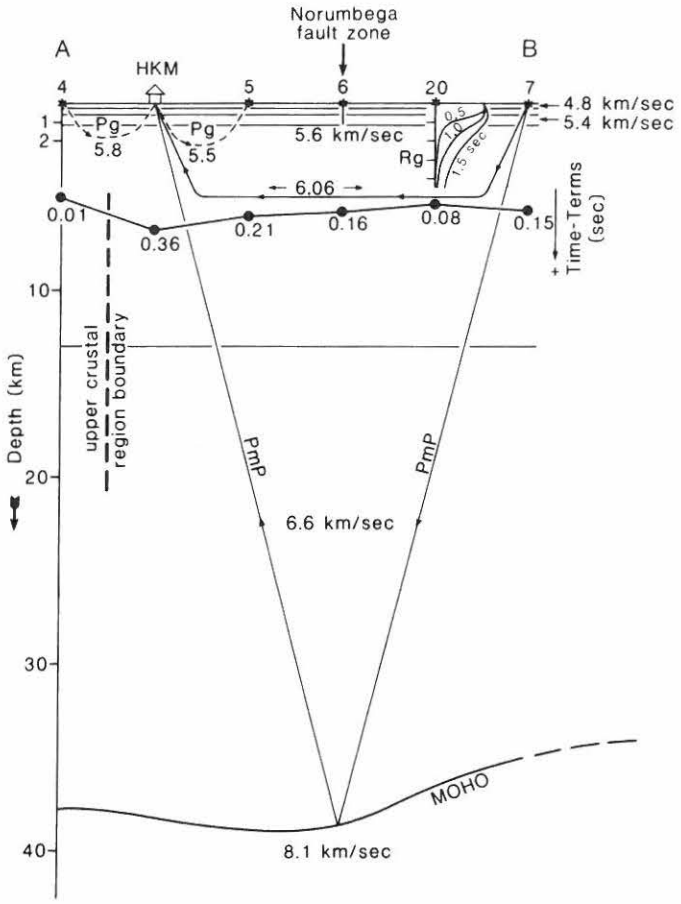

Figure 9b. Schematic diagram of cross-section AB in figure 9a illustrating the relationship between the various wave types and methods used in this study. Vertical exaggeration is approximately 3 to 1. Time-term residuals are plotted in upper crustal layer, and they indicate lower V_p and/or a thicker layer. The curves labelled Rg represent displacement versus depth for Rg waves at periods of 0.5, 1.0 and 1.5 sec.

the P waves generally match well with the velocities found from the surface waves at about the expected bottoming depths of the body waves. The average V_p for one very short path near MIM which bottomed at very shallow depth was 4.9 km/sec. That result compares well with values obtained for the top layers of the slow and average Rg models. The rest of the average V_p measurements indicate a range of 5.5 to 6.3 km/sec for V_p at about 2 or 3 km depth, and the surface wave results range from 5.6 to 6.6 km/sec for V_p at a depth of about 2 km. The assumed V_p/V_s ratio (discussed below) and the assumed bottoming point of the body waves are not accurate enough to conclude whether the differences in these two ranges are significant. Third, anisotropy does not appear to exist near station TRM nor in coastal Maine east of Penobscot Bay. However, Doll et al. (1986) argued that there may be anisotropy in the vicinity of shotpoints 10 and 11, and the fast average velocity parallel to the Appalachians to station JKM could support that argument. Fourth, the velocities in easternmost Maine are, on average, greater than those in any of the areas to the west and northwest. This is consistent with the Pg time-term results, even though different data were used in the two analyses. It is curious that the velocities found for paths from shotpoint 26 are not significantly slower than those for other nearby shotpoints. This suggests that the source of the slow anomaly found in the Pg time-term analysis lies deeper than 2 or 3 km in the crust or is directly beneath the shotpoint. Finally, the average velocity from shotpoint 4 to HKM is significantly faster than that from shotpoint 5 to HKM, evidence that the sharp change in the time-term residuals in this area has some expression in very shallow parts of the crust.

A more detailed comparison of body wave and surface wave results can be obtained for the slow Rg paths by comparing the results of Kafka and Reiter (1987) with those of Klemperer and Luetgert (1987) for essentially the same path (Fig. 6c here and Profile 1 of their study). Based on that comparison, it appears that the V_p/V_s ratio used by Kafka and Reiter (1987) is too low and that a value of about 1.9 may be more appropriate.

DISCUSSION OF RESULTS

Relationship Between Lithotectonic Terranes and Regions with Distinct Seismic Structure

In this section, we discuss the relationship between our seismic results and locations of distinct lithotectonic terranes in the study area. The concept of lithotectonic terranes has been applied to the northern Appalachians by a number of authors, notably Williams and Hatcher (1982) and Keppie (1985). Lithotectonic terranes are crustal blocks of distinct stratigraphy, structure, petrology, metamorphism, and paleomagnetics with a geologic history different from that of adjacent terranes until some juxtaposing or suturing event occurred. In Maine, Williams and Hatcher (1982) defined three major terranes, from northwest to southeast: the Dunnage, the Gander, and the Avalon. Keppie (1985) argued that each of these are in fact accumulations of several terranes and should be considered superterranes. In Maine, he defined a number of terranes including the Boundary composite terrane, itself an accumulation of several terranes, in the northwestern part of the Gander superterrane. South of the Fredericton-Norumbega fault he identified a number of individual terranes within the Avalon superterrane, and he grouped this with the Meguma superterrane of Williams and Hatcher (1982) into the Acadia composite terrane (called here the Acadia composite/Avalon terrane, see Fig. 7). The Boundary composite terrane probably assembled in late Cambrian or early Ordovician and is thought to have accreted to the North American margin along with the rest of the Gander superterrane during Ordovician time (Keppie, 1985). According to paleomagnetic evidence, the Acadia composite/Avalon terrane had amalgamated by early Cambrian time and then underwent 1500 km of sinistral movement relative to the North American craton (Keppie, 1985; Kent and Opdyke, 1978; Kent, 1982). This movement was proposed to have taken

place during mid-Cretaceous time (Kent, 1982), but reexamination of the paleomagnetic evidence has moved this date back to at least the early Permian and significantly reduced the earlier-calculated offset (Kent and Opdyke, 1984).

Four regions of differing seismic characteristics can be generally delineated from our seismic results (see Fig. 11). The first region is in Canada where the two shotpoints show negative time-term residuals. These two shotpoints, both of which occur outside of the primary source/receiver area, are poorly sampled, each having only a few rays and a restricted range of approach azimuths. Thus, it is not clear whether these negative values represent real travel-time variations under the sites or whether they merely demonstrate an inadequecy of the tomographic time-term method for sites at the periphery of the experiment area. The second region extends from the Maine-Quebec border southeast to the central cross line of the USGS experiment (shotpoints 12 through 17). In this region, the time-term residuals generally scatter around zero. A few more positive time-term residuals occur in the area of the Boundary composite terrane in northwestern Maine. Generally, small time-term residuals would be expected for northwestern Maine from the upper-crustal velocity model along the northern cross line (shotpoints 8 through 11) reported by Doll et al. (1986). The more positive time-term residuals may represent real velocity or structure variations, or they could be an artifact of the anisotropy proposed for this area (Doll et al., 1986). The third region is that of generally larger, positive time-term residuals between HKM and the coast and between shotpoints 18 and 22. From the surface-wave and body-wave results presented in this study and those of Klemperer and Luetgert (1987), there appears to be a strong upper-crustal anisotropy (as much as 10%) in this region with the fast velocity direction being parallel to the regional trend of the geologic structure. The positive time-term residuals and the slow refractor block in this region may be due to the rather large angles with which a number of the Pg ray paths cross the regional structure. This region crosses the Norumbega fault zone from the Gander superterrane into the Acadia composite/Avalon terrane. The fourth region lies east of shotpoint 22 along coastal Maine. The Pg time-term residuals show a great variation but are generally consistent with the direct P-wave velocity measurements which show faster crust on average than that immediately to the west. Such a relationship between the two regions has also been noted by Klemperer and Luetgert (1987). There does not appear to be any strong anisotropy in this last region, which corresponds roughly to the St. Stephen terrane of Keppie (1985).

In general, the sharpest differences in seismic structure occur at the edge of and within the Acadia composite/Avalon terrane. Since the seismically slow crust in the Penobscot Bay region crosses the Norumbega fault, it seems unlikely that the Norumbega fault accounts for the strike-slip offset required by the paleomagnetic data. Such a fault would be expected to have an expression at the crustal depths sampled in this seismic analysis. Ludman (1986) has also argued for this interpretation of the Norumbega fault zone based on geologic evidence.

Correlation of Time-term Results with Gravity and Magnetic Anomalies

It is interesting to compare the Pg tomographic time-term results with the regional gravity and magnetic fields. There appears to be a correspondence between the tomographic time-term results and the Bouguer gravity field in Figure 10. More negative Bouguer anomaly values generally correlate with more negative time-term residuals, while more positive anomalies occur where there are more positive time-term residuals. The positive time-term residuals in northwestern Maine follow a ridge in the gravity field, a feature which is associated with the Boundary composite terrane. The sharp change in the time-term residuals to larger positive values southeast of shotpoint 4 occurs precisely at a step in the gravity field. This feature, known as the central Maine gravity gradient, stretches northeast into Canada where it is exposed at the surface in the Kingman fault zone (Ludman, 1986). Strong variations in the time-term residuals in easternmost Maine are coincident with a zone of rapidly changing gravity anomalies and of numerous plutonic bodies. Shotpoint 26 with its large positive time-term lies atop the western edge of a strong gravity gradient. Both the seismic and the gravity observations are due to contrasts located within the upper third of the crust.

The aeromagnetic field in Maine (Zietz et al., 1980) does not match the seismic results nearly as well as the gravity field does. This is not surprising since rocks of different density and elastic properties need not have different magnetic properties.

Implications for Models of Tectonic Evolution of the Crust Underlying Maine

The similarity of the seismic properties of the upper crust across the Norumbega fault zone as determined from the body-wave and surface wave analysis supports the arguments of Kent and Opdyke (1984) and Ludman (1986) that the Norumbega fault zone is not a major, post-Acadian megashear. On the other hand, the differences in the seismic properties of the upper crust between shotpoint 4 and HKM and between shotpoints 22 and 23 indicate the possibility of terrane boundaries at these localities. In the first case, the change in seismic properties occurs at the central Maine gravity gradient. This is also the location of the Kingman fault zone, a feature argued by Ludman (1986) to be a pre-Silurian suture. In the second case, the change occurs at the western edge of the coastal volcanic belt, a locality which has been suggested to be a terrane boundary (Klemperer and Luetgert, 1987).

The present-day evolution of the crust underlying Maine is expressed primarily by the seismicity of the region (Fig. 11). There is widespread activity in the southwestern part of the state, while more concentrated pockets of activity occur in the central and eastern areas. Except for a few small earthquakes which have been observed, northern Maine is the most seismically quiet part of the state. In central Maine there may be a tendency for earthquakes to occur in the vicinities of the boundaries

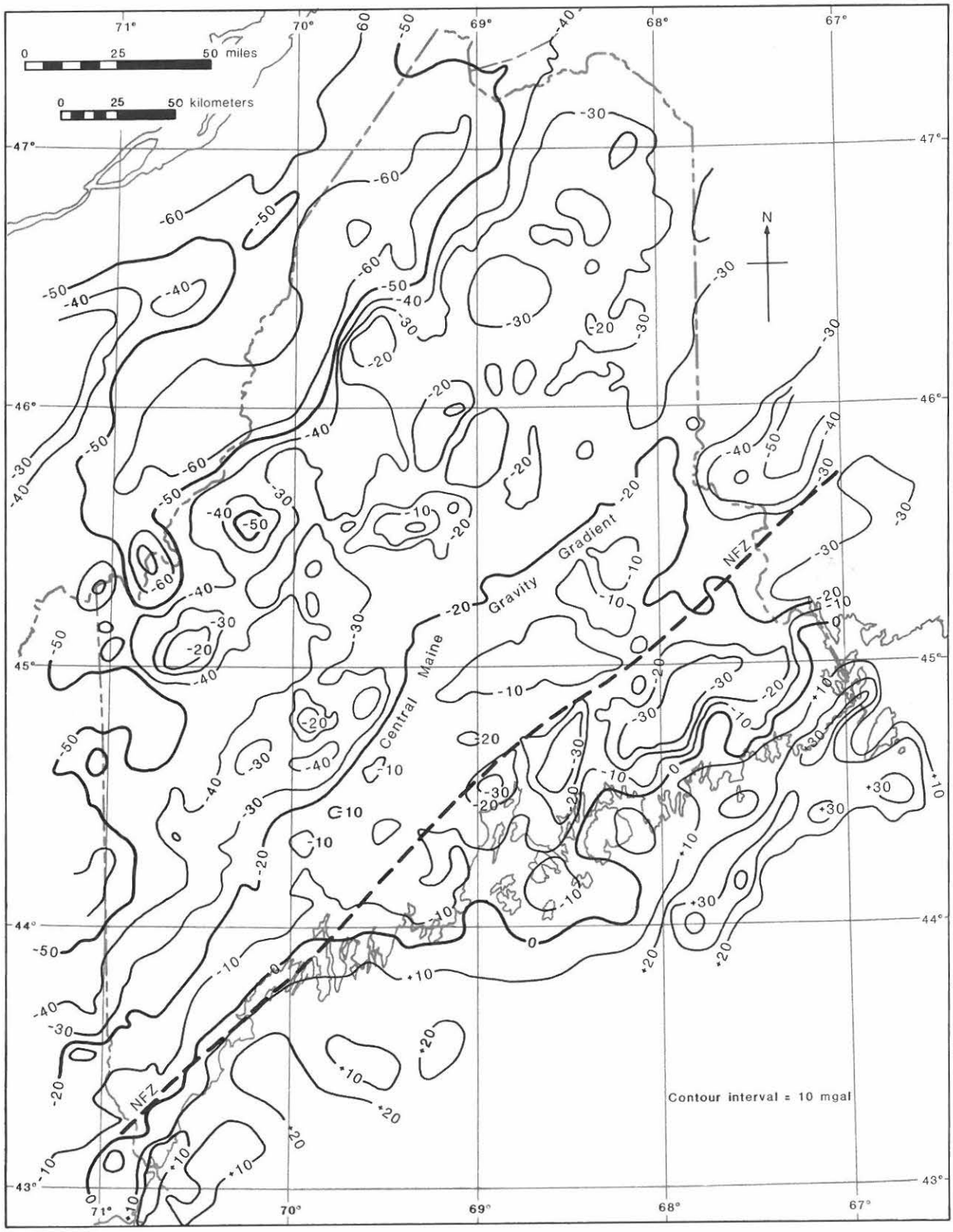

Figure 10. Bouguer gravity anomalies in the state of Maine (adapted from Haworth et al., 1980).

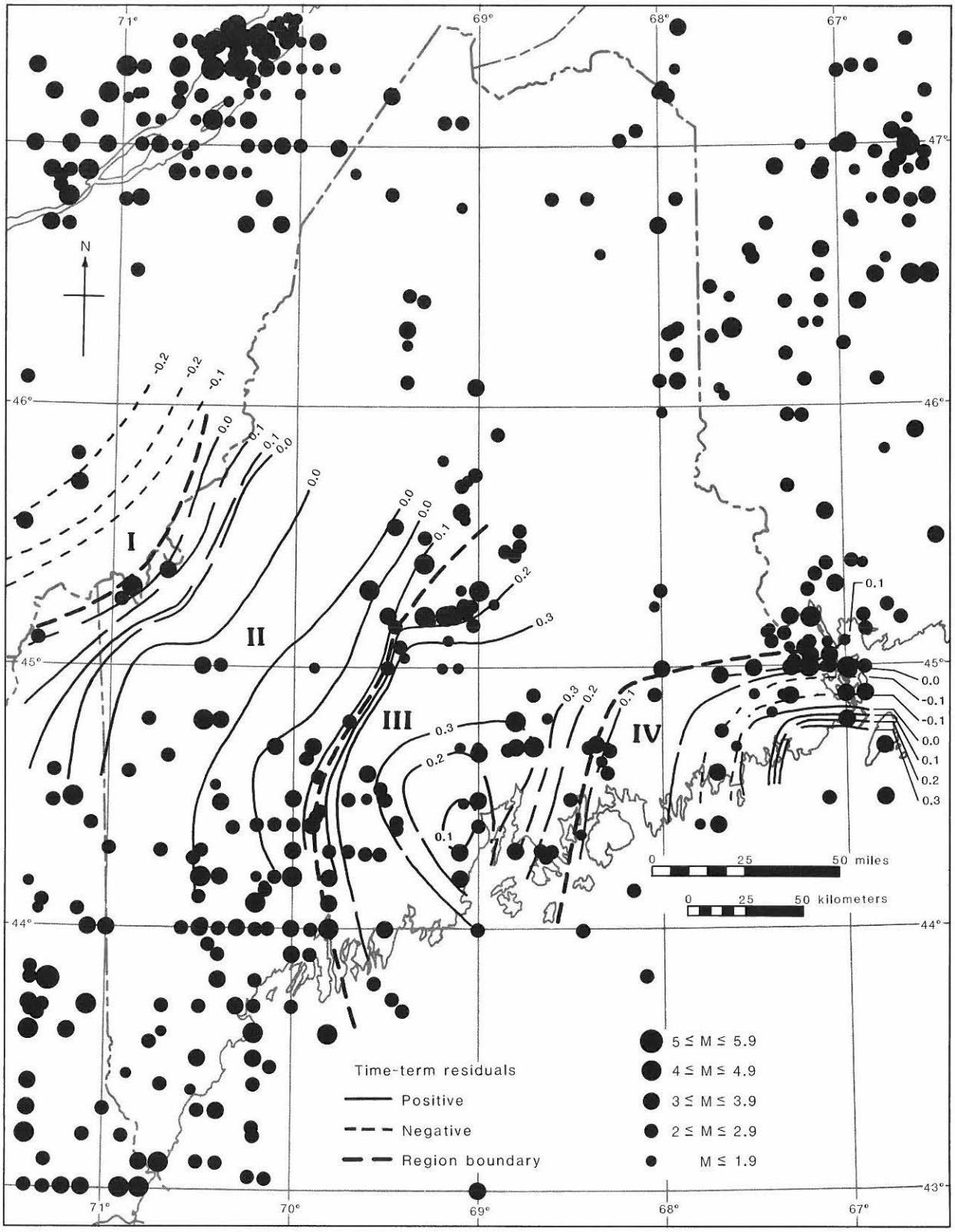

Figure 11. Geophysical basement terranes determined from the Pg time-term analysis. Also plotted are epicenters of earthquakes located in Maine for the period 1534-1985. Dashed lines indicate boundaries of four regions of different upper crustal seismic structure found in this study (I, II, III, and IV).

of the geophysically different regions found in this study (Fig. 11). For example, there is some indication of a band of seismicity that trends northeast from the southwest corner of Maine to the international border in east-central Maine. Such a trend would approximately follow the trend of the central Maine gravity gradient. Thus, some of the present-day earthquake activity could be due to the reactivation of a terrane boundary in the basement rocks by the modern tectonic stress field. The inability to identify presently active faults in the surface geology (Ebel, 1983; Ebel and McCaffrey, 1984; Ebel, 1986) may be an indication that it is in the basements blocks beneath the Paleozoic cover rocks that the now-active zones of weakness associated with the earthquakes can be found.

ACKNOWLEDGMENTS

Some of the research presented in this paper is based on work supported by the North Atlantic Treaty Organization under a grant awarded to J. E. Ebel. Operation of the New England Seismic Network was supported by the U.S. Nuclear Regulatory Commission under Grant NRC 5-23678-179. Research support for this study was also provided by the Air Force Office of Scientific Research under Grant AFOSR 85-0177, and by the National Science Foundation under Grant EAR-8606404.

REFERENCES CITED

Backus, G., and Gilbert, F., 1970, Uniqueness in the inversion of gross earth data: Phil. Trans. Roy. Soc. London., Ser. A, v. 266, p. 123-192.

Bullen, K. E., 1963, An introduction to the theory of seismology, 3rd edition: Cambridge University Press, New York.

Chiburis, E. F., and Ahner, R. O. (eds.), 1980, Northeastern U.S. Seismic Network Bulletin No. 15, Seismicity of the Northeastern United States, April 1, 1979 - June 30, 1979: Weston Observatory, Boston College, Weston, MA.

Der, Z., Masse, R., and Landisman, M., 1970, Effects of observational errors on the resolution of surface waves at intermediate distances: J. Geophys Res., v. 75, p. 3399-3409.

Doll, W. E., Luetgert, J. H., and Murphy, J. M., 1986, Seismic refraction and wide-angle reflection profiles in the northern Appalachians: the Chain Lakes Massif, northwest Maine: EOS, Trans. Am. Geophys. Un., v. 67, p. 312.

Dziewonski, A. M., Bloch, S., and Landisman, M., 1969, A technique for the analysis of transient seismic signals: Seism. Soc. Am., Bull., v. 59, p. 427-444.

Ebel, J. E., 1983, A detailed study of the aftershocks of the 1979 earthquake near Bath, Maine: Earthquake Notes, v. 54, no. 4, p. 27-40.

Ebel, J. E., 1985, A study of seismicity and tectonics in New England: U.S. Nuclear Regulatory Commision, NUREG/CR-4354, 88 p.

Ebel, J. E., 1986, A study of seismicity and tectonics in New England: Technical progress report, 1 April 1985 - 31 March 1986: submitted to U.S. Nuclear Regulatory Commission, 12 p.

Ebel, J. E., and McCaffrey, S. J., J. P, 1984, The Mc=4.4 earthquake near Dixfield, Maine: Earthquake Notes, v. 55, no. 3, p. 21-24.

Eichorn, S. J., 1980, A refraction study of northern New England: M.S. thesis, Boston College, Chestnut Hill, MA, 66 p.

Fawcett, J. A., and Clayton, R. W., 1984, Tomographic reconstruction of velocity anomalies: Seism. Soc. Am., Bull., v. 74, p. 2201-2219.

Franklin, J. N., 1972, Well-posed stochastic extension of ill-posed linear problems: J. Math. Anal. & Appl., v. 31, p. 681-716.

Green, A. G., Berry, M. J., Spencer, C. P., Kanasewich, E. R., Chiu, S., Clowes, R. M., Yorath, C. J., Stewart, D. B., Unger, J. D., and Poole, W. H., 1986, Recent seismic reflection studies in Canada, *in* Barazangi, M., and Brown, L. (eds.), Reflection seismology: a global perspective: Am. Geophys. Un., Geodynamics Series, v. 13, p. 85-97.

Haworth, R. T., Daniels, D. L., Williams, H., and Zeitz, I., 1980, Magnetic anomaly map of the Appalachian orogen: Mem. Univ. of Newfoundland, Map No. 3.

Hearn, T., and Clayton, R. W., 1986a, Lateral velocity variations in southern California, I. Results for the upper crust from Pg waves: Seism. Soc. Am., Bull., v. 76, p. 495-509.

Hearn, T., and Clayton, R. W., 1986b, Lateral velocity variations in southern California, II. Results for the lower crust from Pn waves: Seism. Soc. Am., Bull., v. 76, p. 511-520.

Kafka, A. L., and Dollin, M. F., 1985, Constraints on the lateral variation in upper crustal structure beneath southern New England from dispersion of Rg waves: Geophys. Res. Lett., v. 12, p. 235-238.

Kafka, A. L., and McTigue, J. M., 1985, The Avalonian terrane and Merrimack trough in southern New England: similarities and differences in upper crustal structure determined from dispersion of Rg waves: (Abs.), EOS, Trans. Am. Geophys. Un., v. 66, p. 987.

Kafka, A. L., and Reiter, E. C., 1987, Dispersion of Rg waves in southeastern Maine: evidence for lateral anisotropy in the shallow crust: Seism. Soc. Am., Bull., v. 77, p. 925-941.

Kent, D. V., 1982, Paleomagnetic evidence for post-Devonian displacement of the Avalon platform (Newfoundland): J. Geophys. Res., v. 87, p. 8709-8716.

Kent, D. V., and Opdyke, N. D., 1978, Paleomagnetism of the Devonian Catskill red beds: evidence for motion of the coastal New England-Canadian Maritime region relative to North America: J. Geophys. Res., v. 83, p. 4441-4450.

Kent, D. V., and Opdyke, N. D., 1984, A revised paleopole for the Mauch Chunk Fm. of the Appalachians and its tectonic implications: (Abs.), EOS, Trans. Am. Geophys. Un., v. 65, p. 200.

Keppie, J. D., 1985, The Appalachian collage, *in* Gee, D. G., and Sturt, B. A. (eds.), The Caledonide orogen – Scandinavia and related areas: John Wiley and Sons, Ltd., New York, p. 1217-1226.

Klemperer, S. L., and Luetgert, J. H., 1987, A comparison of reflection and refraction processing and interpretation methods applied to conventional refraction data from coastal Maine: Seism. Soc. Am., Bull., v. 77, p. 614-630.

Ludman, A., 1986, Timing of terrane accretion in eastern and east-central Maine: Geology, v. 14, p. 411-414.

Luetgert, J. H., 1985a, Lithospheric structure in the northern Appalachians from the 1984 Maine-Quebec seismic refraction data: (Abs.), EOS, Trans. Am. Geophys. Un., v. 66, p. 308.

Luetgert, J. H., 1985b, Depth to Moho and characterization of the crust in the northern Appalachians from 1984 Maine-Quebec seismic refraction data: (Abs.), EOS, Trans. Am. Geophys. Un., v. 66, p. 1074-1075.

Luetgert, J. H., and Bottcher, C., 1987, Seismic refraction profiles within the Merrimack synclinorium, central Maine: (Abs.), EOS, Trans. Am. Geophys. Un., v. 68, p. 347.

Luetgert, J. H., Mann, C. E., and Klemperer, S. L., 1987, Wide-angle deep crustal reflections in the northern Appalachians: Geophys. J. R. Astr. Soc., v. 89, p. 183-188.

Luetgert, J. H., Stewart, D. B., Hutchinson, D. R., and Spencer, C. P., 1986, Northern Appalachian crustal transect: (Abs.), EOS, Trans. Am. Geophys. Un., v. 67, p. 1097.

Mann, C. E., and Luetgert, J. H., 1985, Seismic refraction data within the Avalonian terrane, eastern Maine: analysis of 2-D structure from normal moveout record sections: (Abs.), EOS, Trans. Am. Geophys. Un., v. 66, p. 987.

McMechan, G. A., and Mooney, W. D., 1980, Asymptotic ray theory and synthetic seismograms for laterally varying structure: theory and application to the Imperial Valley, California: Seism. Soc. Am., Bull., v. 70, p. 2021-2035.

Mitchell, B. J., and Herrmann, R. B., 1979, Shear velocity structure in the eastern United States from inversion of surface wave group and phase velocities: Seism. Soc. Am., Bull., v. 69, p. 1133-1148.

Murphy, J. M., and Luetgert, J. H., 1986, Data report for the Maine-Quebec cross-strike seismic refraction profile: U.S. Geol. Surv., Open-File Report 86-47.

Murphy, J. M., and Luetgert, J. H., in press, Data report for the 1984 Maine along-strike seismic refraction profile: U.S. Geol. Surv., Open-File Report.

Nakanishi, I., 1985, Three-dimensional structure beneath the Hokkaido-Tohoku region as derived from a tomographic inversion of P-arrival times: J. Phys. Earth, v. 33, p. 241-256.

Nakanishi, I., and Anderson, D. L., 1983, Measurement of mantle wave velocities and inversion for lateral heterogeneity and anisotropy, I: J. Geophys. Res., v. 88, p. 10267-10283.

Nutting, M., 1984, A synthetic seismogram study of New England crustal models: M.S. thesis, Boston College, Chestnut Hill, MA, 78 p.

Osberg, P. H., Hussey, A. M., II, and Boone, G. M., 1985, Bedrock geologic map of Maine: Maine Geol. Surv., scale 1:500,000.

Santo, M., 1965, Lateral variation of Rayleigh waves dispersion character, Part II: Eurasia: P. A. Geoph., v. 62, p. 67-80.

Sheriff, R. E., and Geldart, L. P., 1982, Exploration seismology, Vol. 1, History, theory and data acquisition: Cambridge University Press, New York.

Spencer, C., Green, A., and Luetgert, J. H., 1987, More seismic evidence on the location of the Grenville basement beneath the Appalachians of Quebec-Maine: Geophys. J. R. Astr. Soc., v. 89, p. 177-182.

Stewart, D. B., Unger, J. D., Phillips, J. D., Goldsmith, R., Poole, W. H., Spencer, C. P., Green, A. G., Loiselle, M. C., and St-Julien, P., 1986, The Quebec-Maine seismic reflection profile: setting and first year results, *in* Barazangi, M., and Brown, L. (eds.), Reflection seismology: the continental crust: Am. Geophys. Un., Geodynamics Series, v. 14, p. 189-200.

Suetsugu, D., and Nakanishi, I., 1985, Tomographic inversion and resolution for Rayleigh wave phase velocities in the Pacific Ocean: J. Phys. Earth, v. 33, p. 345-368.

Suzuki, Z., 1964, Maine seismic experiment: a study of shear waves: Seism. Soc. Am., Bull., v. 55, p. 425-439.

Taylor, S. R., and Toksoz, M. N., 1979, Three-dimensional crust and upper mantle structures of the northeastern United States: J. Geophys. Res., v. 84, p. 7627-7644.

Taylor, S. R., and Toksoz, M. N., 1982, Structure of the northeastern United States from inversion of Rayleigh wave phase and group velocities: Earthquake Notes, v. 53, p. 5-24.

Unger, J. D., Stewart, D. B., and Phillips, J. D., 1987, Interpretation of migrated seismic reflection profiles across the northern Appalachians in Maine: Geophys. J. R. Astr. Soc., v. 89, p. 183-188.

Williams, H., and Hatcher, R. D., Jr., 1982, Suspect terranes and accretionary history of the Appalachian orogen: Geology, v. 10, p. 530-536.

Woodhouse, J. H., and Dziewonski, A. M., 1984, Mapping the upper mantle: three-dimensional modeling of earth structure by inversion of seismic waveforms: Jour. Geophys. Res., v. 89, no. B7, p. 5933-5986.

Zietz, I., Haworth, R. T., Williams, H., and Daniels, D. L., 1980, Magnetic anomaly map of the Appalachian orogen: Mem. Univ. of Newfoundland, Map No. 2.